Preliminary geochemical investigation of a possible CO_2 injection in the Ungaran geothermal field, Indonesia: equilibrium and kinetic modeling

Gagas Pambudi Utomo (iD) **and Nilgün Güleç**, Middle East Technical University, Çankaya, Ankara, Turkey

Abstract: Carbon capture and storage (CCS) is considered to be an effective method to mitigate anthropogenic carbon emissions that have been the major cause of global warming. One of the possible sites to store CO_2 is in geothermal reservoirs. In this study, an attempt to simulate CO_2–brine reservoir rock interaction inside a geothermal reservoir is carried out using the PHREEQC program. The study utilizes published rock mineralogy of the assumed reservoir lithology and chemistry of the hot water in the Ungaran geothermal field, Java, Indonesia. The simulation is based on equilibrium and kinetic modeling and assumes a single stage CO_2 injection kept at a constant temperature and pressure. The amount of injected CO_2 is determined by solubility modeling of CO_2 in hot water under estimated reservoir conditions. The modeling predicted (i) the effect of solubility trapping at early stages of CO_2–brine rock interaction, (ii) dissolution of Ca-bearing silicates (plagioclases) coupled with calcite precipitation as a potential chemical processes relevant to a possible CO_2 mineralization, (iii) progressive transition from solubility to mineral trapping becoming significant after 30 days following injection, (iv) minor porosity increase ($\sim$0.5%), and (v) achievement of equilibrium between CO_2–brine-rock in 10 years after injection. Sensitivity analysis associated with the uncertainties for altering mineral proportion and rock porosity reveal no significant change in the ability of the modeled reservoir to trap injected CO_2 into mineral phases. Concerning the CCS studies so far carried out in geothermal fields in volcanic reservoirs, this modeling comprises one of the first performed for fields with intermediate volcanics. The result from this study can be utilized as foreknowledge for possible future CCS operations in Indonesian geothermal fields. © 2020 Society of Chemical Industry and John Wiley & Sons, Ltd.

Keywords: CO_2 storage; geothermal reservoir; equilibrium modeling; kinetic modeling

Introduction

One of the methods considered effective to reduce CO_2 emission is CO_2 capture and storage (CCS) which involves capturing CO_2 produced at large industrial facilities and power plants, and storing it in subsurface geologic formations.[1] The possible storage sites include depleted oil/gas fields,[2–4] deep saline aquifers,[5–7] unmineable coal seams,[8,9] and basaltic rocks.[10–12] One of the main concerns of CCS is the long-term safety of CO_2 fixation which occurs via two mechanisms: physical and geochemical trapping.[13] The first one consists of static (structural and stratigraphic), hydrodynamic, and residual gas trapping. The second, which is considered to be the safest means of fixation, is separated into solubility and mineral trapping[14] in which the injected CO_2 is converted into permanent aqueous and immobile carbonates, respectively. Depleted oil/gas fields and deep saline aquifers are generally characterized by major dissolution and minor mineralization of injected CO_2,[2] while basaltic rocks in volcanic geothermal fields demonstrate rapid mineralization of injected CO_2.[15] An example of CO_2 capture and subsequent storage in basaltic geothermal reservoirs is the Hellisheidi geothermal field (CarbFix Project, Iceland).[16]

Indonesia, as a major carbon emitter, has been developing its CCS program in the past 11 years.[17–22] The first project which is still in progress is the Gundih CCS pilot project.[23–27] Studies suggest that depleted oil/gas field and saline aquifers are potential storage sites in the country but face challenges due to their remoteness from CO_2 sources.[18,22] In addition to these sites, the abundance of geothermal fields with intermediate volcanic reservoir lithology[28] as potential CO_2 storage sites is yet to be investigated. Indonesia is currently the second largest geothermal energy producer in the world having a total installed capacity of 1925 MW with most of these fields located close to CO_2 sources in Java and Sumatra Islands.[29] The development of CCS in geothermal fields[12,13,15,16] consequently makes Indonesia a potential leader in testing and potentially demonstrating this technology. Further, the reservoir rock in most geothermal fields in Indonesia comprises volcanics with intermediate composition[30] consisting of active silicate minerals (source of Ca^{2+}, Mg^{2+}, and Fe^{2+}) required for carbonate formation.[31] Although successful CCS operations have only been conducted in geothermal fields with basaltic reservoirs,[13,15,16] experimental studies of CO_2 storage in intermediate and felsic reservoirs have also been attempted.[32–34] Due to their relatively short distance to CO_2 sources and theoretically compatible lithology for CO_2 storage,[32,33] Indonesian geothermal fields have a potential to become possible future CO_2 storage sites and thus a preliminary study to support such an idea is required.

Considering the importance of solubility and mineral trapping for long-term safety of CO_2 storage,[13,14] assessment of both mechanisms through geochemical study is common prior to CCS operations. Such assessments can be achieved through monitoring, experimental laboratory studies, and geochemical modeling of CO_2–brine rock interaction. Noble gas and stable isotope monitoring studies in natural gas fields,[2] deep saline aquifers,[35] depleted oil fields,[36–37] and geothermal fields as natural analogues of CO_2 storage sites[38] identify solubility as the dominant chemical trapping mechanism, and suggest a minor role for mineral trapping. This observation is further supported by experimental studies,[39] which also point to the effect of pH and CO_2 pressure on the carbonate formation.[40] Other laboratory studies draw attention to the usability of noble gases to track CO_2 migration.[41] Geochemical modeling to forecast long-term effect of CO_2 storage using programs such as PHREEQC,[42] is also conducted because laboratory studies are unable to reconstruct CO_2 storage over geologic time scales. Several researchers have demonstrated the ability of the PHREEQC program in simulating: dissolution and precipitation of minerals after CO_2 injection,[43,44] calculation of CO_2 trapped as minerals,[45] interaction of CO_2-rich brine with calcite,[46] CO_2–brine rock interaction in siltstone and sandstone dominated oil reservoir.[47] In the case CO_2 storage in volcanic geothermal reservoirs, previous geochemical modeling study is limited to investigating the interaction of CO_2-saturated water with basaltic reservoir.[48] Study related to intermediate reservoir is yet to be observed despite the fact that CO_2 fixation varies considerably with the varying mineral assemblages in different rock types.

Given, (i) the potential of geothermal fields in Indonesia to be utilized as CO_2 storage sites and (ii) the importance of geochemical studies related to CO_2–brine rock interaction prior to CO_2 injection, this study aims to perform preliminary investigation of a possible future CO_2 storage in the Ungaran geothermal field near the industrial city of Semarang which is predicted to annually emit 22 409 kt CO_2 by 2030.[49]

Figure 1. Geographic setting of the Ungaran geothermal field.

This is achieved by modeling CO_2–brine rock interaction using published rock mineralogy of assumed reservoir lithology and chemistry of hot spring sample presumed to represent reservoir water. These data are used as input for reaction with (theoretically injected) CO_2 under reservoir pressure and temperature condition using PHREEQC program, and the effect of CO_2 injection is evaluated to assess solubility and mineral trapping. In order to promote immediate solubility of injected CO_2,[12,13] the amount of injected CO_2 is taken as the maximum amount of CO_2 per liter brine that may dissolve under estimated reservoir condition and is determined by solubility modeling of CO_2. The simulation is based on

equilibrium and kinetic modeling and assumes a single stage CO_2 injection under a constant temperature and pressure in a static environment. Ultimately, the attempted modeling and its results will provide an example for other preliminary CCS studies in Indonesian geothermal fields.

Ungaran geothermal field
Geographic setting and geology
The Ungaran field comprises one of the several geothermal fields in the Java island (Fig. 1) and is situated in the southern flank of Ungaran volcano (Fig. 2). This volcano has an elevation of 2050 m and is
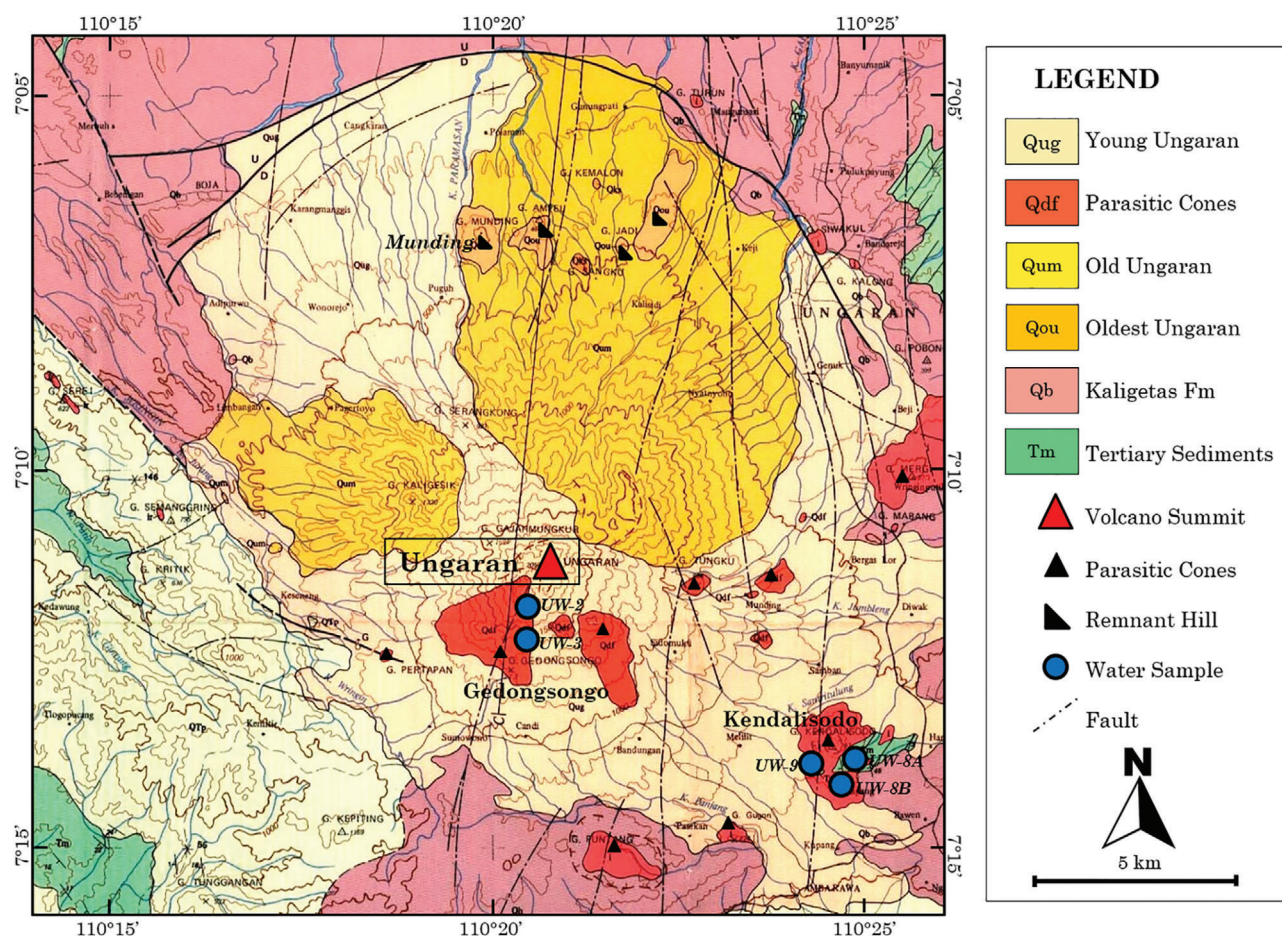
Figure 2. Geological map of the Ungaran Volcano, Java Island, Indonesia. Redrawn after Thanden *et al.*,[53] Phuong *et al.*,[51] and Putranto and Rude.[50]

located 30 km south of Semarang city in Central Java province, Indonesia. Tertiary marine sediments comprising of Banyak, Kapung, Damar, and Kalibeng formations are present at the base of Ungaran volcano (Fig. 2). These units are overlain by Kaligetas formation formed during early Pleistocene which consists of lava flows, breccia, claystone, and tuffaceous sandstone.[50,51] The Ungaran volcano is characterized by three stages of growth: oldest Ungaran, old Ungaran, and young Ungaran. Oldest Ungaran was formed from submarine activity during early Pleistocene. Erosion of oldest Ungaran produced five remnants hills with Munding hill (Fig. 2) being the most elevated. Old Ungaran was formed during middle Pleistocene comprising of basaltic, basaltic andesitic, and andesitic lavas.[52] Collapse of old Ungaran formed a caldera and is followed by the growth of several parasitic cones with Kendalisodo (Fig. 2) being the most noticeable.[53] Young Ungaran was formed during late
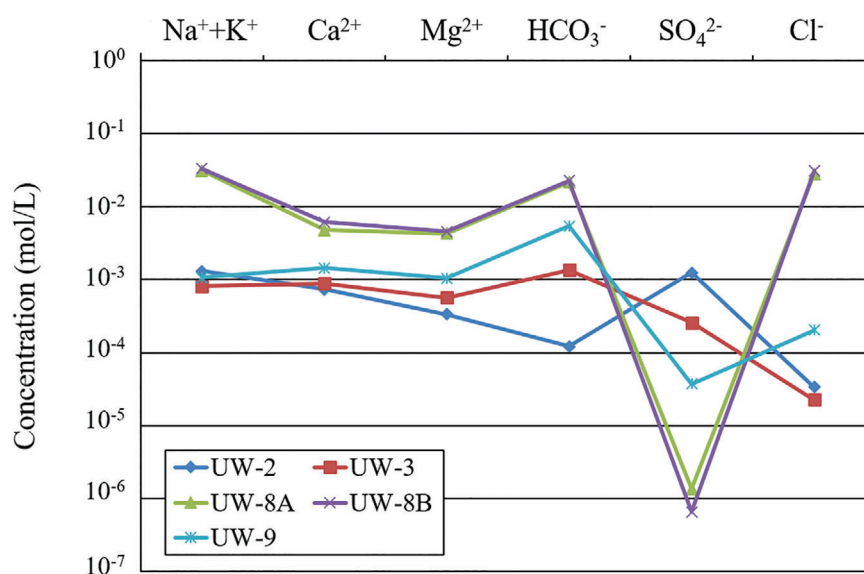
Pleistocene–early Holocene inside the caldera produced from subsidence of old Ungaran. Young Ungaran is characterized by andesitic lava, perlitic lava, and volcanic breccia.[52] Structural analysis of this area revealed that the Ungaran volcanic system is controlled primarily by the occurrence of the Ungaran collapse structure running from the northwest to the southeast. Fault systems trending northwest to southeast and northeast to southwest control the old volcanic rocks of the precaldera formation.[54]

Brine and reservoir rock properties

The Ungaran geothermal field is related with the recent young Ungaran volcanism. Gedongsongo and Kendalisodo are the main geothermal areas (Fig. 2) located on the southern flank of the Ungaran volcano.[55] The composition of thermal spring waters at Ungaran geothermal field reveals the presence of two water types: the acid-sulfate water type which

ID	T(°C)	pH	K$^+$	Na$^+$	Ca^{2+}	Mg^{2+}	SiO$_2$	HCO$_3^-$	SO$_4^{2-}$	Cl$^-$	TDS
UW-2	40	5.4	8.6	25.3	32.6	10.3	109	59	136	1.2	383
UW-3	56	6.1	7.9	14.1	37.1	15.1	86	200	31.8	0.8	393.5
UW-8A	35.2	6.8	44.2	700	217.3	117.7	92	1732	0.2	998	3917.4
UW-8B	38.1	6.8	47.1	746	278.4	126	95	1824	0.1	1088	4224.4
UW-9	23.8	7.9	2.4	23.2	62.1	26.9	51	351	4.4	7.2	528.4

Table 1. Brine chemistry (in mg L^{-1}) of Ungaran geothermal field waters[51].

Figure 3. Schoeller diagram of waters from the Ungaran geothermal field, Java Island, Indonesia. Data source: Phuong *et al.*[51]

originates from steam heated meteoric water located near the volcano summit and neutral bicarbonate water type located at lower altitude.[56] The chemical compositions of water samples of Ungaran geothermal field denoted by UW[51] are given in Table 1 and are depicted in terms of a Schoeller diagram in Fig. 3. The first two samples, UW-2 and UW-3, are from Gedongsongo region in southern flank of Ungaran volcano. The other three, UW-8A, UW-8B, and UW-9 are located in Kendalisodo region (See Fig. 2). UW-2 is classified as alkali-calcium-sulphate (Na+K-Ca-SO$_4$) water, UW-3 and UW-9 are calcium-bicarbonate (Ca-HCO$_3$) water, UW-8A and UW-8B are alkali-chloride-bicarbonate (Na+K-HCO$_3$-Cl) type water. Reservoir temperature estimates from silica geothermometers range between 72–143°C.[51]

Precaldera volcanics (oldest and old Ungaran volcanics) and the tertiary marine sedimentary rocks are considered to be the main geothermal reservoir rocks of Ungaran geothermal field.[56,57] The volcanic rocks are characterized by 48.90–60.80% SiO$_2$, and

classified as trachyandesite to trachybasaltic andesite consisting mainly of plagioclase, sanidine and cristobalite.[51,52] Quartz, halloysite and alunite are the main secondary minerals reported in the hydrothermal alteration zones of the field, along with minor chlorite and calcite.[51,52] The geothermal reservoir is estimated to be at 1000–3500 m depth.[54]

Geochemical modeling

Modeling has been done using PHREEQC program to simulate CO$_2$-brine rock interaction under reservoir condition and evaluate the composition changes in brine and rock after CO$_2$ injection. PHREEQC is freeware which performs a wide variety of aqueous geochemical calculations and is used for modeling reactions and processes, including (1) speciation and saturation-index calculations and (2) batch reaction.[42] The modeling has been implemented by using, as inputs, (i) chemistry and temperature of hot-spring sample presumed to be the most representative of
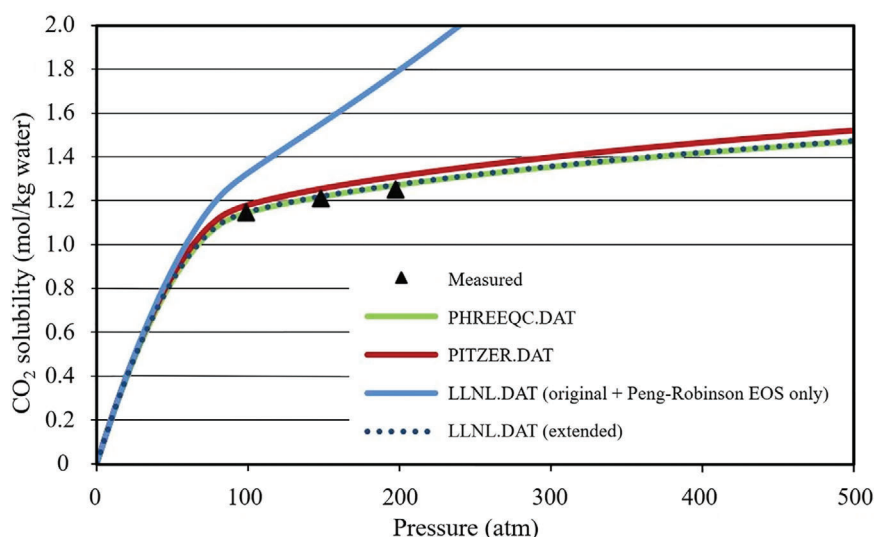
Figure 4. CO_2 dissolution in a 0.35 mol kg^{-1} water NaCl solution at 40°C taken from Klajmon *et al.*[47] and the references therein.

reservoir water, (ii) depth, porosity and normative mineralogy of the assumed reservoir rock lithology, and (iii) the amount of injected CO_2 based on solubility modeling of CO_2 in hot water under the estimated reservoir conditions. The modeling assumes a single stage CO_2 injection kept under a constant temperature and pressure. Due to the limited study of reservoir characteristics (permeability, flow regime), and how previous modeling studies are conducted,[32–34,47] the modeling has been done in a static environment where there is no mass flow occurring in the simulated reservoir. The constant temperature assigned corresponds to the reservoir temperature and constant pressure corresponds to the hydrostatic pressure present at the reservoir depth.

The thermodynamic extended llnl.dat database has been used in the PHREEQC program during simulation. In a previous study, it is reported that the phreeqc.dat, pitzer.dat, and llnl.dat are unable to predict the solubility of CO_2 in a higher-pressure environment (Fig. 4).[47] Thus, redefinition of CO_2 dissolution reaction was needed and additional parameters from phreeqc.dat is extended into the llnl.dat database to overcome this limitation. Modeling has been performed in two separate batch namely equilibrium and kinetic modeling. From both modeling studies, the fate of injected CO_2 has been evaluated by observing the compositional change in the brine chemistry and the rock mineralogy.

CO_2–brine rock interaction starts, following injection of CO_2, with dissolution (solubility trapping) which leads to pH drop that produces variation in species concentration of brine. This process promotes dissolution of alkali earth metals, which then reacts with dissolved C-bearing species to form carbonates (mineral trapping).[58] Once CO_2–brine rock interaction reached equilibrium state, the final composition of brine and rock have been evaluated to assess solubility and mineral trapping (equilibrium modeling). The changes observed from the beginning of injection until equilibrium state have been further studied to better understand the process affecting the two trapping mechanisms (kinetic modeling).

Modeling inputs

Given that (i) some of the waters are reported to be products of mixing with cold groundwater[51] and (ii) mixing yields underestimated silica geothermometry results, a further attempt to estimate reservoir temperature has been made in this study using silica-enthalpy mixing model (Fig. 5). This calculation yielded an enthalpy range of 699–1000 kJ kg^{-1} corresponding to a temperature range of 166–233°C. During simulation, temperature of reservoir has been assigned a value of 200°C. The main reservoir unit has been assigned to be the old Ungaran volcanics which is reported to be within the depth of 1000 and 3500 m below surface at the geothermal prospect area with an average rock density of 2640 g cm^3.[54] Given that the reservoir depth is between 1000–3500 m, reservoir
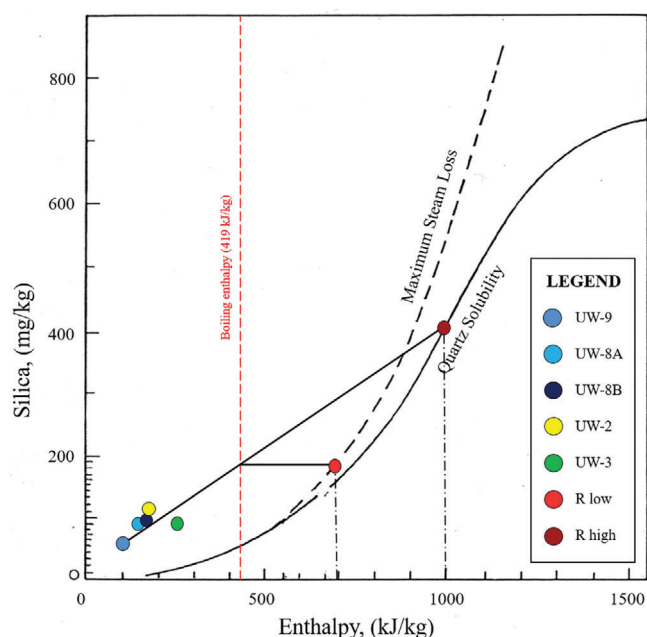
Figure 5. Silica-enthalpy mixing diagram of the Ungaran waters. Maximum reservoir temperature (R high) is estimated from the intersection of mixing line between cold water and hot water with quartz solubility curve assuming no steam separation. Minimum reservoir temperature (R low) is predicted from the intersection of mixing line and boiling enthalpy line with solubility curve for maximum steam loss.

pressure has been assigned as 249 atm corresponding to hydrostatic pressure at depth of 2500 m.

Since no drilling has yet been performed in the field that would provide opportunity to have access to the rock samples (drill cores or cuttings) representative of reservoir rock mineralogy, the published major element chemistry of old Ungaran volcanics [52] has been converted to normative mineralogy which is achieved by the use of CIPW norms. This normative mineralogy is comprised, by volume, of 15.70% quartz, 24.47% anorthite, 21.04% albite, 20.61% orthoclase, 3.13% corundum, 13.35% enstatite, 0.77% ilmenite, 0.64 apatite, and 0.02% zircon. Taking into account the observation of the previous researchers [51] that there are secondary minerals in the reservoir lithology, 10% volume fraction of alteration minerals (halloysite, alunite, and quartz) has been added to the normative mineralogy obtained by CIPW Norm calculation, and the data have been renormalized to 100% to represent the reservoir rock mineralogy shown in Table 2. Taking into account that the old Ungaran volcanics are located in the same volcanic belt as Awibengkok field, which is one of the major geothermal fields in Java (Fig. 1), the

porosity has been taken to be 0.10 similar to that of Awibengkok reservoir.[59]

Given that the highest concentration levels are recorded in sample UW-8B (Table 1), this sample has been taken to represent the water composition of Ungaran geothermal field. Injected CO₂ has been kept in dissolved state to prevent potential leakage due to CO₂ bouyancy.[60] In order to maintain CO₂ in dissolved state, the ratio of CO₂ to H₂O should be kept less than the solubility of CO₂ at reservoir condition.[61] Solubility of CO₂ in brine (UW-8B) is simulated using PHREEQC at various pressure values and the assigned temperature of 200°C (473.15 K). This simulation has identified the approximate solubility of CO₂ in UW-8B sample at 473.15 K and 249 atm as 1.5 mol kg⁻¹ water. Consequently, 1.4 mol of CO₂ has been assigned during modeling. Modeling assumes a single stage CO₂ injection during simulation under a constant temperature and pressure in a static environment. Equilibrium and kinetic modeling assumes that 1 L of brine fills the entire pore space of the reservoir and the volume of reservoir rock is adjusted accordingly. Volume fractions of minerals have been converted to mol by using density of the rock and the molar weight of minerals (Table 2).

Equilibrium modeling

Brine and reservoir rock have been equilibrated with CO₂ to calculate expected final reservoir composition after equilibrium phase is achieved in the system CO₂–brine rock. Since simulation has been done in static environment, in which no mass transfer occurs during simulation, total brine plus reservoir rock volume is conserved. Porosity change has been calculated by subtracting the final porosity from the initial porosity assigned as 0.10. Final porosity of reservoir rock has been calculated by subtracting the final volume of rock from the conserved total brine plus rock volume (10 000 cm³). Final volume of rock can be obtained using Eqn (1):

$$V_{final} = \sum \frac{M_f \cdot GFW_i}{\rho} \qquad (1)$$

Where GFW_i and M_f are the molar weigth (g mol⁻¹) and final amount (mol) of a single mineral, respectively. The symbol ρ is the rock density (g cm⁻³). Secondary carbonates (calcite, dolomite, ankerite, dawsonite, magnesite, siderite) have been included in the simulation to evaluate possible mineral trapping mechanism for CO₂ fixation in the reservoir. Given the

Table 2. Reservoir rock mineralogy used as input in geochemical modeling.

Mineral	(Chemical formula)	[a]Volume fraction (%)	[b]Renormalized volume fraction (%)	GFW (g mol^{-1})	[c]Amount (mol)	[d]SSA (m^2 g^{-1})
Quartz	SiO$_2$	15.70	17.47	60.08	69.09	0.80[47]
Anorthite	CaAl$_2$Si$_2$O$_8$	24.47	22.27	277.41	19.07	0.02[47]
Albite	NaAlSi$_3$O$_8$	21.04	18.94	263.02	17.11	0.02[47]
Orthoclase	KAlSi$_3$O$_8$	20.61	18.55	278.33	15.83	0.31[47]
Corundum	Al$_2$O$_3$	3.13	2.82	101.96	6.56	3.70[64]
Enstatite	MgSiO$_3$	13.35	12.02	100.39	28.44	9.30[65]
Ilmenite	FeTiO$_3$	0.77	0.69	151.71	1.09	0.20[66]
Apatite	Ca$_5$(PO$_4$)$_3$F	0.64	0.58	504.30	0.27	–
Zircon	ZrSiO$_4$	0.02	0.02	603.61	0.01	–
Halloysite	Al$_2$Si$_2$O$_5$(OH)$_4$	–	3.33	258.16	3.06	20.00[47]
Alunite	KAl$_3$O$_8$(SO$_4$)$_2$(OH)$_6$	–	3.33	414.21	1.91	26.00[67]
Calcite	CaCO$_3$	–	–	100.10	–	0.15[47]
Dolomite	CaMg(CO$_3$)$_2$	–	–	184.4	–	0.18[47]
Ankerite	CaMg$_{0.3}$Fe$_{0.7}$(CO$_3$)$_2$	–	–	206.39	–	–
Dawsonite	NaAlCO$_3$(OH)$_2$	–	–	144	–	–
Magnesite	MgCO$_3$	–	–	84.31	–	–
Siderite	FeCO$_3$	–	–	115.86	–	–
Anhydrite	CaSO$_4$	–	–	138.15	–	0.12[47]
Gypsum	CaSO$_4$•2H$_2$O	–	–	138.15	–	–

[a] Mineral volume fraction obtained from CIPW Norm calculation.
[b] Renormalized mineral volume fraction after 10% alteration mineral addition.
[c] Amount of minerals converted from volume fraction in b.
[d] Specific Surface Area (SSA).

presence of sulphate type waters in the field (UW-2),[51] anhydrite and gypsum have been also included in the modeling studies.

Result of equilibrium modeling has been assessed based on the changes in brine chemistry, mineral composition, and porosity value of the reservoir rock. Equilibrium modeling results (Table 3) showed complete dissolution of halloysite and alunite, and a partial dissolution of anorthite. Minor dissolution of albite was also noted. Quartz, corundum, and orthoclase, as well as secondary minerals (calcite and anhydrite) appeared to precipitate. The amounts of enstatite, ilmenite, apatite, and zircon remain unchanged. There seemed to be a minor increase in reservoir rock porosity from its initial value of 0.1–0.106. The introduction of CO$_2$ lead to the precipitation of calcite which can be suggested as the mineral trapping mechanism in the field. Regarding the brine chemistry, pH seemed to increase from 6.80 to 7.17. There was also a significant increase in sulfate (SO$_4$$^{2-}$) and decrease in magnesium and bicarbonate (Mg^{2+}, HCO$_3$$^-$) concentrations in the brine chemistry (Fig. 6) .

Kinetic modeling

Kinetic modeling has been performed to evaluate the change in mineral composition for an interval of time as the interaction between CO$_2$–brine reservoir rock proceeds. The modeling has been based on dissolution rate of minerals. The dissolution of minerals is defined by Eqn (2).

$$r_i = A_i \cdot GFW_i \cdot M_i \cdot \left(1 - \frac{Q_i}{K_i}\right) \cdot \left(k_{i(acid)} + k_{i(neutral)}\right)$$

$$\left(+ k_{i(base)} + k_{i(carbonate)}\right) \tag{2}$$

Table 3. Results of equilibrium modeling showing the change in the mineral composition of reservoir rock after CO₂ injection.

Mineral	(Chemical formula)	Mineral amount (mol)		
		Initial	Final	Delta
Quartz	SiO_2	69.09	79.98	10.89
Anorthite	$CaAl_2Si_2O_8$	19.07	13.82	−5.25
Albite	$NaAlSi_3O_8$	17.11	17.10	−0.01
Orthoclase	$KAlSi_3O_8$	15.83	17.74	1.91
Corundum	Al_2O_3	6.56	16.78	10.22
Enstatite	$MgSiO_3$	28.44	28.45	0.01
Ilmenite	$FeTiO_3$	1.09	1.09	0.00
Apatite	$Ca_5(PO_4)_3F$	0.27	0.27	0.00
Zircon	$ZrSiO_4$	0.01	0.01	0.00
Halloysite	$Al_2Si_2O_5(OH)_4$	3.06	0.00	−3.06
Alunite	$KAl_3O_8(SO_4)_2(OH)_6$	1.91	0.00	−1.91
Calcite	$CaCO_3$	0.00	1.43	1.43
Anhydrite	$CaSO_4$	0.00	3.82	3.82

The symbol r_i is the reaction rate (mol s^{-1}), A_i is the specific surface area (m² g^{-1}), GFW_i is the molecular weight (g mol^{-1}) and M_i is the amount (mol) relevant to the mineral. The symbol Q_i denotes activity product, and K_i is equilibrium constant of the mineral. The character k_i is the Arrhenius rate constant

(mol m^{-2} s^{-1}) of a mineral. Arrhenius rate k_i of minerals is divided into several mechanisms: acid, neutral, base, and carbonate mechanisms.[62] Due to the lack of published studies on precipitation rates of minerals, reaction rates of mineral precipitation has been assumed to be defined by the same formula as mineral dissolution. Specific surface area of simulated minerals has been compiled from various works in Table 2. A code to let mineral precipitate with an initial surface area of 0.00001 m² has been assigned to the program.[63] Simulation has been done for 100 years period.

Result from kinetic modeling has been evaluated based on the changes occurring in mineral composition and brine chemistry over a period of time. As for mineral composition, the dissolution and precipitation of reactive minerals (quartz, anorthite, albite, orthoclase, corundum, halloysite, alunite, calcite, and anhydrite) have been examined and depicted as a diagram in Fig. 7 where amount of minerals have been plotted (in units of mol) against time after injection. It appeared from Fig. 7 that dissolution of anorthite, albite, and alunite, and precipitation of quartz, orthoclase, and corundum, occurred immediately after simulation started. Within the time interval 4–36 days after injection (time interval III, 0.01–0.1 year) quartz and corundum precipitation, and anorthite dissolution were in progress, while orthoclase seemed to have
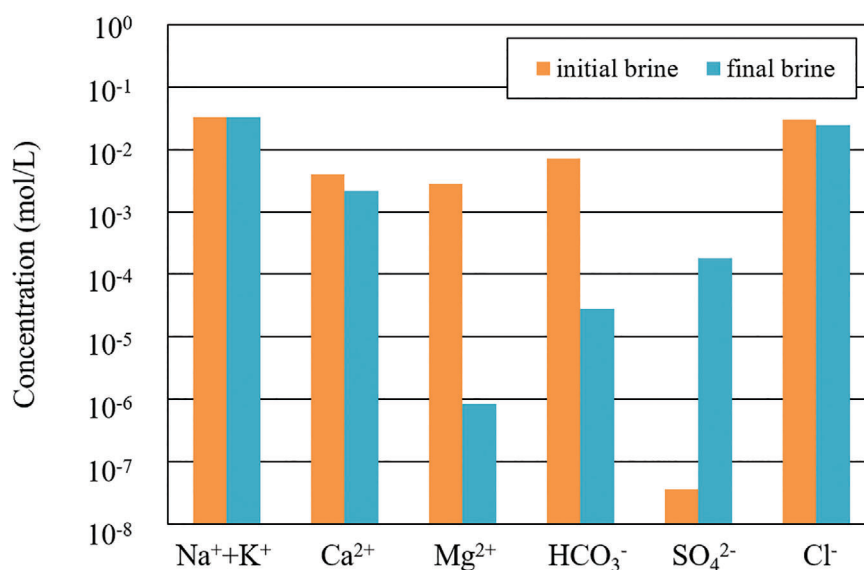

Figure 6. Composition of initial and final brine chemistry. Orange bar indicates the initial brine composition simulated (from the values in Table 1 and Fig. 3) to the assigned reservoir condition, 200°C and 249 atm. Blue bar shows the final composition of brine at equilibrium state among CO₂–brine rock.
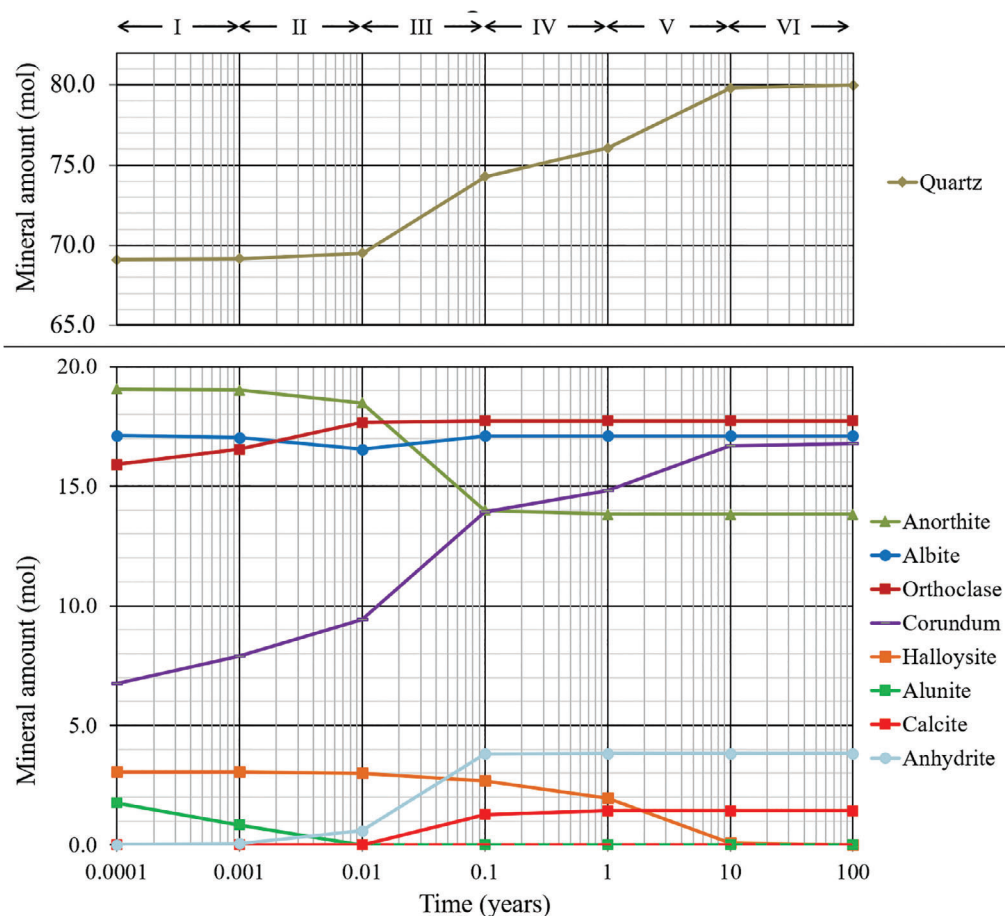
Figure 7. Change in the amount of reservoir minerals against time after CO_2 injection. The Roman numbers refer to the time intervals mentioned in text (note that the profiles point to dissolution for anorthite, halloysite, and alunite, and precipitation for orthoclase, corundum, calcite, and anhydrite).

reached equilibrium in the system and alunite dissolved completely. Between 4–365 days after injection (time interval III and IV, 0.01–1 year) dissolution of anorthite paralleled the precipitation of corundum, anhydrite, and calcite. During the same period, quartz continued its precipitation. Halloysite started to dissolve about 36 days after injection (time interval IV, 0.1–1 year) and became totally dissolved in about 10 years.

Regarding the brine chemistry, the modeling results showed complete dissolution of 1.4 mol CO_2/kg water in the first hour of simulation leading to the maximum dissolved CO_2 amount in the brine (Fig. 8). This value decreased gradually to its minimum value after 1 year. Dissolved CO_2 in brine lowered the pH during the first 10 hours, followed by a progressive pH increase until the end of the first year (Fig. 8).

Discussion

Equilibrium and kinetic modeling predicted the formation of calcite (as a secondary mineral) after CO_2 injection (Table 3 and Fig. 7), indicating a reaction between CO_2 and dissolved Ca^{2+} released solely from silicate minerals in reservoir rocks since no significant drop in Ca^{2+} of brine after equilibrium is observed (Fig. 6). The profiles displayed by anorthite and calcite in Fig. 7 supports this inference pointing to the precipitation of the latter at the expense of the former. This is in line with the conclusion of a previous study[32] that Ca^{2+} can be easily released from silicates of volcanic reservoir rocks and be removed as $CaCO_3$ once it is reacted with hot water and CO_2. On the other hand, Al^{3+} released from the silicate minerals, as well as from the sulphate mineral alunite, appears to have
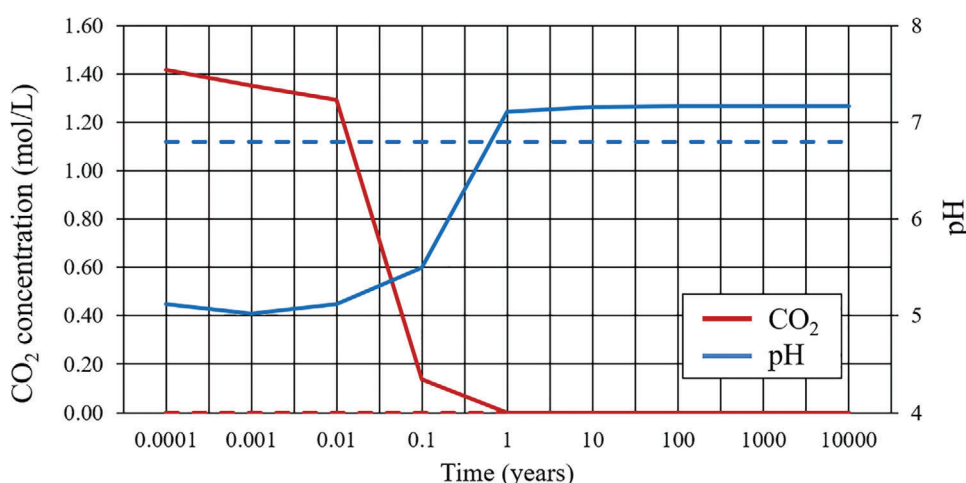
Figure 8. Evolution of injected CO_2 solubility and pH in brine simulated for 100 years period. Dashed lines represent the initial dissolved CO_2 and pH values.

been used for the precipitation of corundum and orthoclase, while the released SiO_2 seems to have increased the amount of quartz. The dissolution of alunite is probably the cause of SO_4^{2-} increase in the brine (Fig. 6), although part of this SO_4^{2-} seems to have been used already for the precipitation of anhydrite (Fig. 7).

Regarding the brine chemistry, the evolutionary trends of CO_2 and pH in Fig. 8 are aligned with common sequential effect of CO_2 dissolution,[58] that is, dissolution of CO_2 in brine lowers the pH at early stages, followed by a progressive pH increase in time. The low pH in the early stage of CO_2-water-rock interaction seems to be responsible for the dissolution of the Ca-bearing silicates (anorthite), as well as alunite (Fig. 7). Kinetic modeling results suggest the occurrence of solubility trapping at the first hour of simulation as shown by the complete dissolution of injected CO_2 in brine (Fig. 8). The contribution of solubility trapping gradually decreases and is replaced by mineral trapping starting from the first hour, but especially significant after 36 days (~0.1 years) of simulation (see Fig. 7). Transition from solubility to mineral trapping is commonly acknowledged by previous studies to take place in tens to thousands of years.[68] However, this timespan depends on the host rock identity and the availability of metallic ions required for precipitation of carbonate minerals, and can be shortened if CO_2 is injected in soluble form rather than gaseous.[61] In this study, complete transition from solubility to mineral trapping occur in the period from 4 days to 1 year after injection. Equilibrium

between CO_2–brine reservoir rock is achieved 10 years after injection (see Fig. 7).

Sensitivity analysis

The results of modeling performed in this study are subject to uncertainties associated with the assumptions regarding the (i) alteration mineral proportion in the mineral assemblage and (ii) rock porosity. The sensitivity analyses related to these uncertainties are given below.

Alteration mineral proportions

The modeling performed in the third section is based on the assumption that 10% of the mineralogic composition is comprised by alteration minerals (alunite, halloysite, quartz [51]). In order to understand the uncertainty associated with this assumption, sensitivity analysis is performed by changing the amount of alteration mineral percentage in modeling. Five batches of equilibrium model are simulated, using 5, 7.5, 10, 12.5, and 15% alteration mineral proportions. Each batch is simulated under the constant pressure and temperature conditions applied, and the same amount of CO_2 specified in the modeling for the field. The result of each batch is analyzed in terms of brine chemistry and rock mineralogy.

In terms of brine chemistry, the variation of alteration mineral abundance has effect only on the final Ca^{2+} and SO_4^{2-} concentrations. The decrease in the final Ca^{2+} and the increase in the final SO_4^{2-} concentrations seems to be enhanced as the proportion
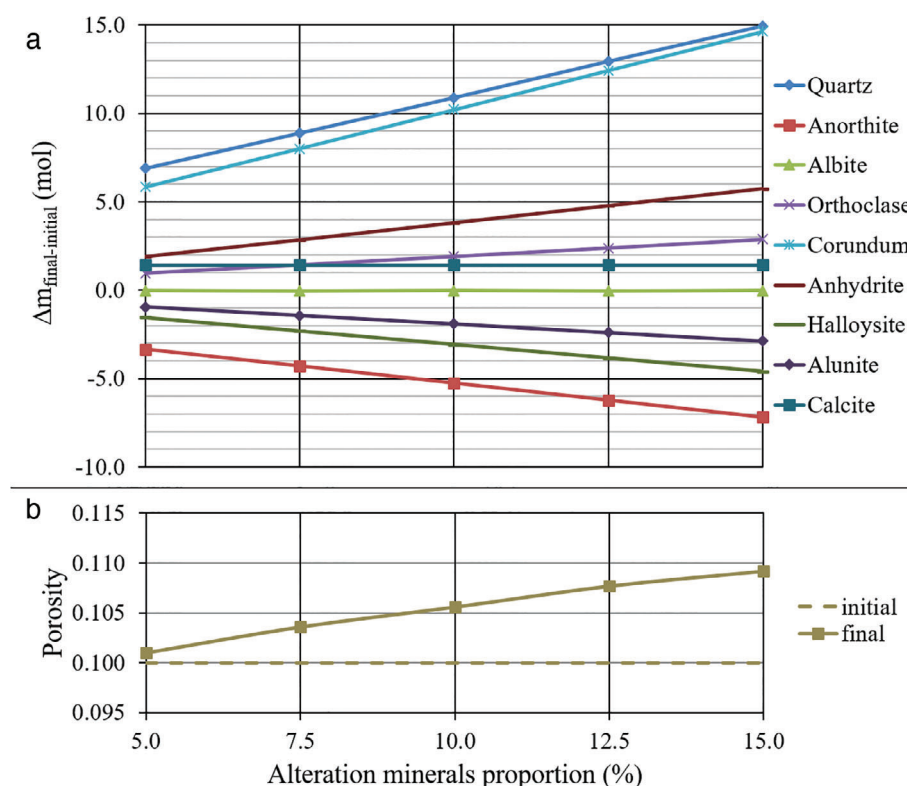
Figure 9. Change in (a) the amount of minerals, (b) in porosity, against the change in the relative proportion of alteration minerals in the assemblage.

of the alteration minerals in the assemblage increases. However, this enhancement does not exceed 0.39 mmol L^{-1} for Ca^{2+}, and 0.018 mmol L^{-1} for SO_4^{2-} for 5% increase in the proportion of the alteration minerals. The pH appears to slightly increase, not exceeding 0.1 unit for 10% increase in the proportion of alteration minerals in the assemblage.

In terms of rock mineralogy, the amount of calcite precipitated is similar (1.4 mol) for all batches (5, 7.5, 10, 12.5, and 15%). Quartz, corundum, orthoclase, and anhydrite precipitate more as the amount of alteration minerals increases (Fig. 9a). Alunite, halloysite, and anorthite seem to be dissolving more with increasing proportion of alteration minerals while no significant trend is observed in albite and calcite (Fig. 9a). In terms of porosity, increase in alteration mineral proportion leads to greater porosity increase (Fig. 9b).

Porosity value

Based on the fact that the Ungaran field has a reservoir lithology comprising of volcanic rocks, and that it is located in the same volcanic zone as Awibengkok field where the measured porosity is 0.10,[59] porosity used in

modeling is taken as 0.10. In order to understand the uncertainty associated with this assumption, sensitivity analysis is performed by changing the porosity value between 0.05 and 0.15. Five batches of equilibrium model are simulated, using 5, 7.5, 10, 12.5, and 15% porosity, under the same conditions specified in the previous section.

In terms of brine chemistry, the variation of porosity has effect on the final Ca^{2+} and SO_4^{2-} concentrations. The decrease in the final Ca^{2+} and the increase in the final SO_4^{2-} concentrations seems to get smaller as the porosity increases. However, this reduction is just about 0.28 mmol L^{-1} for Ca^{2+}, and 0.012 mmol L^{-1} for SO_4^{2-} for 5% increase in porosity. pH value slightly decreases with increasing porosity but does not exceed 0.1 unit for 10% increase in porosity.

In terms of rock mineralogy, the amount of calcite precipitated is similar (1.4 mol) for all batches (5, 7.5, 10, 12.5, and 15%). Quartz, corundum, orthoclase, and anhydrite precipitate less, while alunite, halloysite, and anorthite dissolve less as the amount of porosity increases (Fig. 10). Albite, and calcite do not display any change with the change in porosity (Fig. 10).
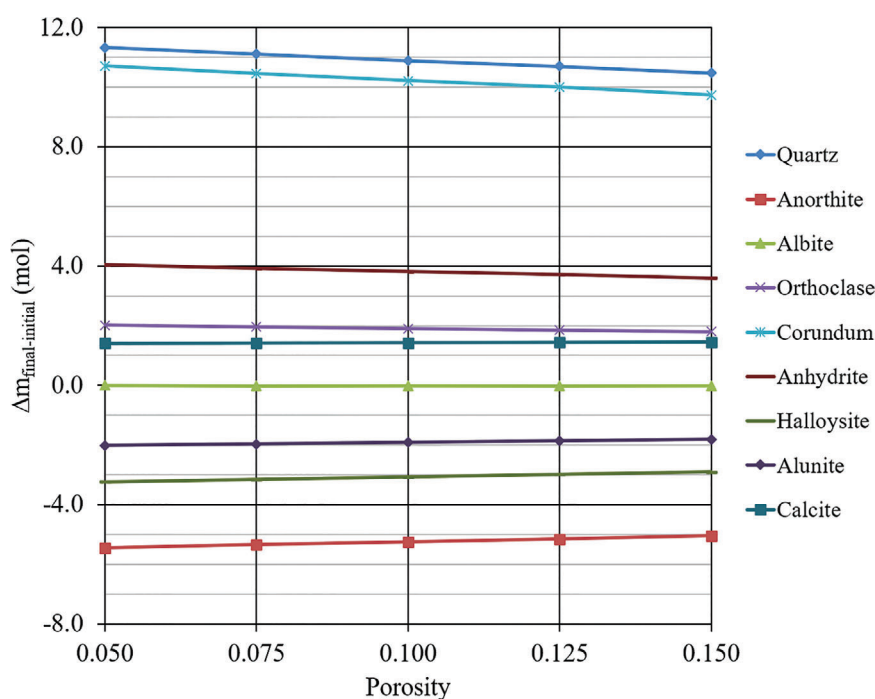
  | *Greenhouse Gas Sci Technol.* 0:1–16 (2020); DOI: 10.1002/ghg.2037

Figure 10. Change in the amount of minerals against the change in porosity.

Limitations and advantages

The simulation performed is limited to static conditions and neglects the effect of mass flow inside a real reservoir environment. This restricts the ability of the simulation to predict spatial impacts of CO$_2$ injection. Reactive transport modeling, which is beyond the scope of the present study, would lead to a better understanding of the fate of CO$_2$, including its spatial evolution at subsurface. Nevertheless, the equilibrium and kinetic modeling carried out in this study provides a useful approach to predict at least the temporal evolution of CO$_2$ in the reservoir. Additionally, because previous geochemical studies on CO$_2$–brine rock interaction are conducted mostly on geothermal reservoirs with basaltic and sedimentary host rocks, the present study is one of the first to focus on intermediate volcanics. The modeling approach outlined in this preliminary study can be used as a guideline for geothermal fields in Indonesia to be considered for future CCS operation.

Concluding remarks

The evolution of theoretically injected CO$_2$ inside the geothermal reservoir of Ungaran field (Indonesia) is simulated using PHREEQC program. The amount of injected CO$_2$ is assigned a value of 1.4 mol kg^{-1} water

as determined by solubility modeling of CO$_2$ in hot water under estimated reservoir conditions, 200°C and 249 atm. The simulation utilizes published data relevant to the reservoir lithology (Ungaran volcanics) and hot water, and is based on equilibrium and kinetic modeling which assumes that 1 L of brine fills the entire pore space of a reservoir with a total volume of 10 L and a porosity of 10%. A further assumption in the modeling is a single stage CO$_2$ injection kept at a constant temperature (200°C) and pressure (249 atm) in a static environment. The modeling results identifies: (i) complete dissolution of CO$_2$ within hours of injection, pointing to the effect of solubility trapping at early stages of CO$_2$–brine rock interaction, (ii) dissolution of anorthite initiated by the dissolution of CO$_2$ and the associated pH lowering in the brine, (iii) precipitation of calcite, at the expense of anorthite dissolution, leading to mineral trapping of CO$_2$, (iv) progressive transition from solubility to mineral trapping which becomes particularly significant in about 30 days following injection, (v) favorable minor porosity increase ($\sim$ 0.5%) in time, and (vi) achievement of equilibrium between CO$_2$–brine rock in 10 years after injection.

Regarding the uncertainties associated with the assumptions relevant to (i) alteration mineral proportion in the mineral assemblage and (ii) rock

porosity, sensitivity analyses reveal that the increase of the first parameter is associated with an increase in the dissolution or precipitation amount of some reactive minerals while an increase in the second parameter is related with lesser dissolution or precipitation amount of these similar reactive minerals taking part in the CO_2–brine rock interaction. However, in terms of carbonate minerals controlling the ability of the geothermal reservoir to trap injected CO_2, there is almost no change in the precipitation amount of calcite which is the sole carbonate mineral in the system. This suggests that the variation in the proportion of alteration minerals and/or porosity does not change the ability of the field to convert CO_2 to mineral phase. However, because the simulation done here is restricted to static environment in which flow regime is neglected, dynamic mass transport study is strongly recommended for future work in order to refine the conclusions obtained from the present study.

Given that the CCS projects in geothermal fields with volcanic reservoirs are limited to basaltic ones, the results from this study can be used for prediction of CO_2 behavior during possible future CCS operations in geothermal fields with intermediate volcanics such as those in Indonesia.

Acknowledgements

Conflict of interest

The authors declare no conflict of interests.

References

1. Captureready, *CCS history*. [Online] (2018). Available at: http://www.captureready.com/EN/Channels/OverViews/showDetail.asp?objID=2&ClassID=1 [November 26, 2018].

2. Gilfillan SMV, Sherwood Lollar B, Holland G, Blagburn D, Stevens S, Schoell M *et al*., Solubility trapping in formation water as dominant CO_2 sink in natural gas fields. *Nature* **458**:614–618 (2009).

3. Underschultz J, Boreham C, Dance T, Stalker L, Freifeld B, Kirste D *et al.*, CO_2 storage in a depleted gas field: an overview of the CO_2CRC Otway Project and initial results. *Int J Greenhouse Gas Control* **5**:922–932 (2011).

4. Györe D, Stuart FM, Gilfillan SMV and Waldron S, Tracing injected CO_2 in the Cranfield enhanced oil recovery field (MS, USA) using He, Ne and Ar isotopes. *Int J Greenhouse Gas Control* **42**:554–561 (2015)..

5. Schilling F, Borm G, Würdemann H, Möller F and Kühn M, CO_2SINK Group, status report on the first European on-shore CO_2 storage site at Ketzin (Germany). *Energy Procedia* **1**:2029–2035 (2009).

6. Nguyen MC, Zhang Y, Li J, Li X, Bai B, Wu H *et al*., A geostatistical study in support of CO_2 storage in deep saline aquifers of the Shenhua CCS project, Ordos Basin, China. *Energy Procedia* **114**:5826–5835 (2017).

7. Ringrose PS, The CCS hub in Norway: some insights from 22 years of saline aquifer storage. *Energy Procedia* **146**:166–172 (2018).

8. Loizzoa M, Lombardi S, Deremble L, Lecampion B, Quesada D, Huet B *et al*., Monitoring CO_2 migration in an injection well: evidence from MovECBM. *Energy Procedia* **4**:5203–5210 (2011).

9. Zhang X and Ranjith PG, Experimental investigation of effects of CO2 injection on enhanced methane recovery in coal seam reservoirs. *J CO2 Util* **33**:394–404 (2019).

10. Goldberg DS, Takahashi T and Slagle AL, Carbon dioxide sequestration in deep-sea basalt. *Proc Natl Acad Sci US A* **105/29**:9920–9925 (2008).

11. Matter JM, Broecker WS, Stute M, Gislason SR, Oelkers EH, Stefansson A *et al*., Permanent carbon dioxide storage into basalt: the CarbFix pilot project, Iceland. *Energy Procedia* **1**:3641–3646 (2009).

12. Gislason SR and Oelkers EH, Carbon storage in Basalt. *Science* **344**(6182):373–374 (2014).

13. Snaebjornsdottir SO, Tomasdottir S, Sigfusson B, Aradottir ES, Gunnarsson G, Niemi A *et al*., The geology and hydrology of the CarbFix2 site, SW-Iceland. *Energy Procedia* **146**:146–157 (2018).

14. Bachu S, Bonijoly D, Bradshaw J, Burruss R, Holloway S, Christensen NP *et al*., CO_2 storage capacity estimation: methodology and gaps. *Int J Greenhouse Gas Control* **1**:430–443 (2007).

15. Gislason SR, Broecker WS, Gunnlaugsson E, Snæbjörnsdóttir S, Mesfina KG, Alfredsson HA *et al*., Rapid solubility and mineral storage of CO_2 in basalt. *Energy Procedia* **63**:4561–4574 (2014).

16. Carbfix, *The CarbFix project* (2018). [Online] Available at: https://www.carbfix.com/carbfix-project [December, 16 2018].

17. Best D, Mulyana R, Jacobs B, Iskandar UP and Beck B, Status of CCS development in Indonesia. *Energy Procedia* **4**:6152–6156 (2011).

18. World Bank, Republic of Indonesia the Indonesia carbon capture storage (CCS) capacity building program: CCS for coal-fired power plants in Indonesia. Report of the World Bank No: ACS14654 (2015). http://documents.worldbank.org/curated/en/563781468284373788/Indonesia-The-Indonesia-carbon-capture-storage-CCS-capacity-building-program-CCS-for-coal-fired-power-plants-in-Indonesia.

19. Darmawan A, Sugiyono A, Liang J, Tokimatsu K and Murata A, Analysis of potential for CCS in Indonesia. *Energy Procedia* **114**:7516–7520 (2017).

20. Usman, Prospect for CO_2 EOR to offset the cost of CCS at coal power plants. *Sci Contributions Oil Gas* **39**(3), 107–118 (2016).

21. Adisaputro D and Saputra B, Carbon capture and storage and carbon capture and utilization: what do they offer to Indonesia? *Front Energy Res* **5**:6 (2017).

22. ADB, Carbon dioxide-enhanced oil recovery in Indonesia: an assessment of its role in a carbon capture and storage pathway. Report of Asian Development Bank, Manila, Philippines. (2019).

23. Tsuji T, Khakim MYN, Kitamura K, Yamada Y, Matsuoka T, Onishi K *et al.*, Gundih CCS project team, CCS project in Gundih gas field, Indonesia (Part 2): reservoir characterization and simulation. Paper presented at the 129th (2013 FALL) Society of Exploration Geophysicists of Japan Conference, Kochi Kaikan, Kochi, Japan. (2013).

24. Kitamura K, Yamada Y, Onishi K, Tsuji T, Chiyonobu S, Sapiie B *et al.*, Gundih CCS project team, potential evaluation of CO₂ reservoir using the measured petrophysical parameter of rock samples in the Gundih CCS project, Indonesia. *Energy Procedia* **63**:4965–4970 (2014).

25. Tsuji T, Matsuoka T, Kadir WGA, Hato M, Takahashi T, Sule MR *et al.*, Reservoir characterization for site selection in the Gundih CCS Project, Indonesia. *Energy Procedia* **63**:6335–6343 (2014).

26. Sule R, Kadira WGA, Matsuoka T, Prabowo H, Sidemen GS, and Indonesia-Japan research team members of Gundih CCS pilot project, Gundih CCS pilot project: current status of the first carbon capture and storage project in South and Southeast Asia regions. Paper presented at 14th International Conference on Greenhouse Gas Control Technologies, Melbourne, Australia. (2018). https://ssrn.com/abstract=3366415.

27. Marbun BTH, Prasetyo DE, Prabowo H, Susilo D, Firmansyah FR, Palilu JM *et al.*, Well integrity evaluation prior to converting a conventional gas well to CO₂ injector well: Gundih CCS pilot project in Indonesia (phase 1). *Int J Greenhouse Gas Control* **88**:447–459 (2019).

28. ESDM, Geothermal investment opportunities in Indonesia. Report of Directorate General of New, Renewable Energy and Energy Conservation. Jakarta: Ministry of Energy and Mineral Resources (2016).

29. Thinkgeo, *Indonesia reaches 1925 MW installed geothermal power generation capacity*. [Online] (2018). Available at: https://www.thinkgeoenergy.com/indonesia-reaches-1925-mw-installed-geothermal-power-generation-capacity/ [June 25, 2020].

30. Purnomo BJ and Pichler T, Geothermal systems on the island of Java, Indonesia. *J Volcanol Geotherm Res* **285**:47–59 (2014.) .

31. Gislason SR, Wolff-Boenisch D, Stefansson A, Oelkers EH, Gunnlaugsson E, Sigurdardottir H *et al.*, Mineral sequestration of carbon dioxide in basalt: a pre-injection overview of the CarbFix project. *Int J Greenhouse Gas Control* **4**:537–545 (2010).

32. Ueda A, Kato K, Ohsumi T, Yajima T, Kaieda H, Ito H *et al.*, Experimental and theoretical studies on CO₂ sequestration into geothermal fields. Proceedings World Geothermal Congress, April 24–29, Antalya, Turkey. (2005).

33. Suto Y, Liu L, Yamasaki N and Hashida T, Initial behavior of granite in response to injection of CO₂-saturated fluid. *Appl Geochem* **22**(1):202–218 (2007).

34. Ré CL, Kaszuba J, Moore J and McPherson B, Supercritical CO₂ in a granite-hosted geothermal system: experimental insights into multiphase fluid-rock interactions. Proceedings

35. of, 37th Workshop on Geothermal Reservoir Engineering, Stanford University, Stanford, CA, January 30—February. (2012).

36. Myrttinen A, Becker V, van Geldern R, Würdemann H, Morozova D, Zimmer M *et al.*, Carbon and oxygen isotope indications for CO₂ behaviour after injection: First results from the Ketzin site (Germany). *Int J Greenhouse Gas Control* **4**:1000–1006 (2010).

36. Lu J, Kharaka YK, Thordsen JJ, Horita J, Karamalidis A, Griffith C *et al.*, CO₂–rock–brine interactions in lower Tuscaloosa formation at Cranfield CO₂ sequestration site, Mississippi, USA. *Chem Geol* **291**:269–277 (2012).

37. Győre D, Gilfillan SMV and Stuart FM, Tracking the interaction between injected CO₂ and reservoir fluids using noble gas isotopes in an analogue of large-scale carbon capture and storage. *Appl Geochem* **78**:116–128 (2017).

38. Güleç N and Hilton DR, Turkish geothermal fields as natural analogues of CO₂ storage sites: gas geochemistry and implications for CO₂ trapping mechanisms. *Geothermics* **64**:96–110 (2016).

39. Wigand M, Carey JW, Schütt H, Spangenberg E and Erzinger J, Geochemical effects of CO₂ sequestration in sandstones under simulated in situ conditions of deep saline aquifers. *Appl Geochem* **23**:2735–2745 (2008).

40. Soong Y, Goodman AL, McCarthy-Jones JR and Baltrus JP, Experimental and simulation studies on mineral trapping of CO₂ with brine. *Energy Convers Manage* **45**:1845–1859 (2004).

41. Kilgallon R, Gilfillan SMW, Edlmann K, McDermott CI, Naylor M and Haszeldine RS, Experimental determination of noble gases and SF6, as tracers of CO₂ flow through porous sandstone. *Chem Geol* **480**:93-104 (2017).

42. Parkhurst DL and Appelo CAJ, Description of input and examples for PHREEQC version 3-A computer program for speciation, batch-reaction, one-dimensional transport, and inverse geochemical calculations. *Denver: U.S. Geological Survey.* [Online] (2013). Available at: https://pubs.usgs.gov/tm/06/a43/ [December 16, 2018].

43. Szabó Z, Hellevang H, Király C, Sendula E, Kónya P, Falus G *et al.*, Experimental modelling geochemical study of potential CCS caprocks in brine and CO₂-saturated brine. *Int J Greenhouse Gas Control* **44**:262–275 (2016).

44. Koukouzas N, Kypritidou Z, Purser G, Rochelle CA, Vasilatos C, and Tsoukalas N, Assessment of the impact of CO₂ storage in sandstone formations by experimental studies and geochemical modelling: The case of the mesohellenic trough, NW Greece, *Int J Greenhouse Gas Control* **71**:116–132 (2018).

45. Király C, Szabó Z, Szamosfalvi Á, Kónya P, Szabó C and Falus G, How much CO₂ is trapped in carbonate minerals of a natural CO₂ occurrence? *Energy Procedia* **125**:527–534 (2017).

46. Steel L, Mackay E and Maroto-Valer MM, Experimental investigation of CO₂-brine-calcite interactions under reservoir conditions. *Fuel Process Technol* **169**:122–131 (2018).

47. Klajmon M, Havlova V, Cervinka R, Mendoza A, Francu J, Berenblyum R *et al.*, REPP-CO₂: equilibrium modelling of CO₂-rock-brine systems. *Energy Procedia* **114**:3364–3373 (2017).

48. Gysi AP and Stefansson A, Experiments and geochemical modelling of CO₂ sequestration during hydrothermal basalt alteration. *Chem Geol* **306–307**:10–29 (2012).

49. Haryono B, Farhan M, Nugroho MLE, Maryono Utama S, Ehara HT, Fujino J *et al.*, Low carbon society scenario

Semarang 2030, [Online] (2017). Available at: https://www.iges.or.jp/en/pub/low-carbon-society-scenario-semarang-2030/en [June 25, 2020].

50. Putranto TT and Rüde TR, Hydrogeological model of an urban city in a coastal area, case study: Semarang, Indonesia. *Indones J Geosci* **3**(1):17–27 (2016).

51. Phuong NK, Harijoko A, Itoi R and Unoki Y, Water geochemistry and soil gas survey at Ungaran geothermal field, central Java, Indonesia. *J Volcanol Geotherm Res* **229–230**:23–33 (2012).

52. Claproth R, Petrography and geochemistry of volcanic rocks from Ungaran, Central Java, Indonesia. Doctor of Philosophy thesis, Department of Geology, University of Wollongong, Australia. (1989).

53. Thanden ER, Sumadirdja H and Richards PW, Geologic map of the Magelang and Semarang Quadrangles, Java. Geological Survey of Indonesia, Scale 1:100,000 (1975).

54. Setyawan A, Ehara S, Fujimitsu Nishijima J, Saibi H and Aboud E, The gravity anomaly of Ungaran Volcano, Indonesia: analysis and interpretation. *J Geotherm Res Soc Japan* **31**(2):107–116 (2009).

55. Hochstein MP and Sudarman S, History of geothermal exploration in Indonesia from 1970 to 2000. *Geothermics* **37**:220–266 (2008).

56. Phuong NK, Hendrayana H, Harijoko A, Itoi R and Unoki R, Geochemistry of the Ungaran geothermal system, Central Java, Indonesia. *Proceedings HAGI-IAGI-PERHAPI Annual Conference and Exhibition 2005*, Surabaya, pp. 64–77 (2005).

57. Saibi H, Aboud E, Setyawan A, Ehara S and Nishijima J, Gravity data analysis of Ungaran Volcano, Indonesia. *Arabian J Geosci* **5**(5):1047–1054 (2011).

58. Elidemir S and Güleç N, Geochemical characterization of geothermal systems in western Anatolia (Turkey): implications for CO$_2$ trapping mechanisms in prospective CO$_2$-EGS sites, *Greenhouse Gas Sci Technol* 1–14 (2017).

59. Stimac J, Nordquist G, Suminar A and Sirad-Azwar L, An overview of the Awibengkok geothermal system, Indonesia. *Geothermics* **37**:300–331 (2008).

60. Burton M and Bryant SL, Surface dissolution: minimizing groundwater impact and leakage risk simultaneously. *Energy Procedia* **1**:3707–3714 (2009).

61. Sigfusson B, Gislason S, Matter J, Stute M, Gunnlaugsson E, Gunnarsson I *et al*., Solving the carbon-dioxide buoyancy challenge: The design and field testing of a dissolved CO$_2$ injection system. *Int J Greenhouse Gas Control* **37**:213–219 (2015).

62. Palandri JL and Kharaka YK, A compilation of rate parameters of water-mineral interaction kinetics for application to geochemical modelling. Open-File Report 2004-1068. Menlo Park, California: U.S. Geological Survey. (2004). https://pubs.usgs.gov/of/2004/1068/.

63. Koenen M, Heege JT and Peeters R, Transport properties of intact caprocks and effects of CO$_2$-water-rock interaction: CO$_2$-induced mineral reactions in sandstone reservoirs (CATO2-WP3.03-D12). CATO-2 project public report. (2014). Available at: https://www.co2-cato.org/cato-download/3773/20141204_095514_CATO2-WP3.03-D12-v2014.10.04-CO2-water-rock-inte .

64. Carroll-Webb SA and Walther JV, A surface complex reaction model for the pH-dependence of corundum and kaolinite dissolution rates. *Geochim Cosmochim Acta* **52**:2609–2623 (1988).

65. Anovitz L, Rondinone A, Sochalski-Kolbus L, Rosenqvist J and Chesire MC, Nano-scale synthesis of the complex silicate minerals forsterite and enstatite. *J Colloid Interface Sci* **495**:94–101 (2017).

66. White AF, Peterson ML and Hochella MF, Electrochemistry and dissolution kinetics of magnetite and ilmenite. *Geochim Cosmochim Acta* **58**(8):1859–1875 (1994).

67. Miller J, Madden A, Phillip-Lander C, Pritchett B and Madden M, Alunite dissolution rates: dissolution mechanisms and implications for Mars. *Geochim Cosmochim Acta* **172**:93–106 (2016).

68. Xu T, Apps JA and Pruess K, Numerical simulation of CO$_2$ disposal by mineral trapping in deep aquifers. *Appl Geochem* **19**(6):917–936 (2004).

Gagas Pambudi Utomo

Gagas Pambudi Utomo is an independent geologist in Bandung, Indonesia. His research fields consist of geothermal systems, geochemistry of geothermal fluids and modeling of CO$_2$-water-rock interaction in subsurface CO$_2$ storage. He received his BSc and MSc degrees from the Department of Geological Engineering, Middle East Technical University, Ankara, Turkey in 2016 and 2019, respectively.

Nilgün Güleç

Nilgün Güleç is a professor in the Geological Engineering Department of the Middle East Technical University (METU), Ankara, Turkey. She received her BSc and MSc degrees from the Department of Geological Engineering, METU, in 1979 and 1982, respectively, and her PhD degree in isotope geochemistry from the Department of Earth Sciences, University of Cambridge (UK) in 1987. She specializes in geochemistry and isotope geology as applied to petrogenesis, ore genesis, and geothermal systems. Particular interest is in geochemical monitoring of geothermal fluids in relation to seismic activities and the assessment of water-rock-CO$_2$ interaction processes in subsurface CO$_2$ storage